

# Entrapment of air at 45° oblique collision of a water drop with a smooth solid surface at room temperature

Hitoshi Fujimoto<sup>\*</sup>, Hirohiko Takuda

*Department of Energy Science and Technology, Graduate School of Energy Science, Kyoto University, Yoshida-Honmachi, Sakyo-ku, Kyoto 606-8501, Japan*

Received 12 July 2003; received in revised form 2 February 2004

## Abstract

This paper treats the oblique impact of a water drop onto a smooth optical glass surface at room temperature. The impact angle between the incoming drop and the surface is 45°. The preimpact diameter of spherical drops is 2.55 mm. The time evolution of the water/solid direct contact area is observed from the reverse side of the impact surface by a flash-photographic technique. It is found that the drop directly contacts the solid surface in a ring shape, and some air is entrapped between the bottom of the drop and the solid surface. Thereafter, a bubble is formed at the impact point. For the case of impact velocity at 1.31 m/s, a fingering pattern is developed from within a ring-shaped wet area, then satellite bubbles in a ring are formed around the bubble at the impact point. No satellite bubble is observed for the case of a higher impact velocity (= 2.11 m/s).

© 2004 Elsevier Ltd. All rights reserved.

*Keywords:* Oblique collision of a drop with a solid; Entrapment of air; Fingering pattern; Satellite bubbles

## 1. Introduction

Under certain impact conditions, when a spherical droplet impinges on a smooth solid surface at room temperature, some air becomes entrapped between the droplet and the solid. Then, an air bubble appears at the liquid/solid interface at the impact point [1–4].

Chandra and Avedisian [1] took clear bird's-eye view photographs of *n*-heptane droplets impacting onto a stainless steel surface at several surface temperatures. In the photographs, a bubble is seen at the impact point. They also showed that satellite bubbles in a ring around the bubble at the impact point appear for relatively high temperatures. Pasandideh-Fard et al. [2] also reported the formation of a single bubble in the impacting droplet

onto a stainless steel surface at room temperature. Thoroddsen and Sakakibara, [3] investigated the fingering-pattern of liquid/solid contact area during the collision of liquid drops with a transparent glass plate. Photographs taken from the reverse side of the solid plate showed that a bubble appears at the impact point after the collision. Fujimoto et al. [4] observed the time evolution of the liquid/solid contact area using a transparent glass plate. The formation process of the single bubble due to the entrapment of air was studied. It should be noted that these studies were conducted using droplets that impinged vertically onto a horizontal smooth surface.

In the present study, the oblique collision of water drops with a dry solid glass surface at room temperature is examined. The impact angle between the incoming drop and the surface is 45°. The preimpact diameter of spherical drops is 2.55 mm, and the impact velocity is varied as a parameter. The time evolution of the water/solid direct contact area is observed from the reverse side of the impact surface by a flash-photographic technique. The effect of impact velocity of drops on the

<sup>\*</sup> Corresponding author. Tel.: +81-75-753-5419; fax: +81-75-753-5428.

E-mail address: [h-fujimoto@energy.kyoto-u.ac.jp](mailto:h-fujimoto@energy.kyoto-u.ac.jp) (H. Fujimoto).

process of air entrapment is investigated. The emphasis is placed on the physics of phenomena at liquid/solid interface in the early stages of the collision.

## 2. Experiments

Fig. 1 shows a schematic of experimental setup, which is based on our previous work [4]. It consists of a reservoir, a needle unit, a catch pan, a triangular prism made of optical glass (BK-7) onto which droplets fall, optical devices (a video camera with a macro lens and a strobe light) to record the deformation behavior of drops, an optical sensor, and a delay timer to trigger the strobe light.

Distilled water at room temperature is used as the test liquid. Water is continuously supplied to the needle unit from a water tank. A drop is formed at the needle, falls because of its own weight, and the next drop appears. This formation process of drops is repeated periodically. The volume of each drop is almost the same and the diameter of spherical drops is 2.55 mm. The impact velocity of drops onto the solid surface varies with the distance between the nozzle and plate.

As shown in Fig. 1, the optical triangular prism is firmly fixed to the base and the inclined angle of the impact surface to the horizontal line is  $45^\circ$ . It should be noted that the flatness of the impact surface, which is defined as the distance between the highest and the

lowest points on the surface in the direction normal to the surface, is 600 nm (specified by manufacturer). The cross section of the prism is an isosceles-right triangle with 15 mm hypotenuse. The area of the surface on which droplets fall is  $300 \text{ mm}^2$  ( $15 \times 20 \text{ mm}$ ).

A laser beam and the optical sensor are set between the needle unit and the impact surface to capture falling drops. The optical sensor gives a trigger signal to the delay timer and operates the strobe light with a preset delay time. Since the video camera with a macro lens is adjusted to effectively record the image only by the light of the flash and the duration of the flash is very short ( $=2 \mu\text{s}$ , specified by the manufacturer), instantaneous images of drops on the solid can be obtained.

The light path originating from the strobe light is depicted by a dotted line in the figure. The light is first reflected at a right angle on the mirror, comes into the prism and reaches the impact surface. The incident angle of the light to the impact surface is approximately  $45^\circ$ . Since the refractive indices of air, water and optical prism are 1.0, 1.33 and 1.52 at wavelength of 589.3 nm, respectively, Snell's law gives the critical angles  $\theta_{\text{air-solid}} = 41^\circ$  at air/solid interface and  $\theta_{\text{water-solid}} = 61^\circ$  at water/solid interface. Thus, total reflection occurs at the dry surface (or air/solid interface). On the other hand, the light is partly reflected at the wet surface (or water/solid interface), and is partly transmitted into water. Consequently, we can take instantaneous photographs of the liquid/solid interface, in which the liquid/solid contact area (wet area) is darker than the liquid/air interface (dry area). However, it should be noted that the wet area is not always dark. For example, let us consider the case where the thin water film covers the solid surface. Light transmitted into the water is totally reflected at the water/air interface and then enters the prism. In such cases, the wet area does not become dark in the photographs. The effect of the light being reflected at the liquid/air interface in the drops cannot be removed from the photographs. Thus, serious attention needs to be paid to the effect of light reflection when the physics of phenomena is discussed.

In the present experiments, if the impact condition is fixed, the collision behavior of drops with the solid surface is expected to be repeatable. Many video images are taken with different delay times under the same impact condition. A sequence of instantaneous photographs showing the collision behavior of drops can be obtained by arranging images of different drops in chronological order. It should be noted that the experimental uncertainty or measurement uncertainty mainly arises from irregularity of formation of drops at the needle unit.

The wet surface is carefully wiped with clean tissues before each test, while the catch pan captures falling drops. Therefore, the drops hit the dry surface at every test.

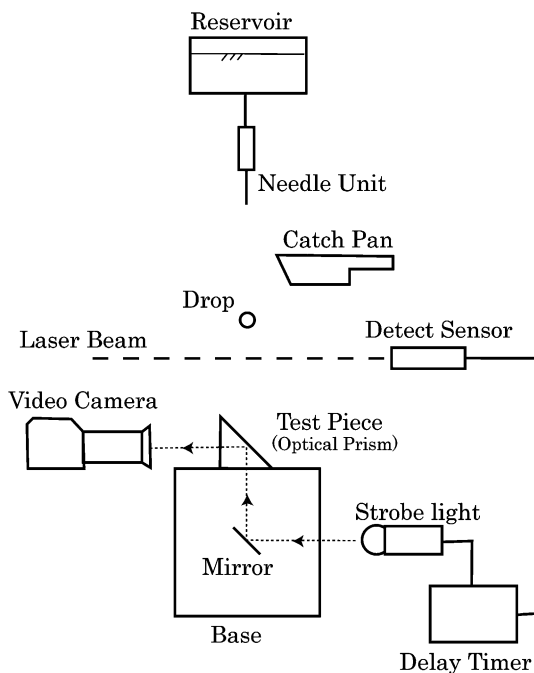


Fig. 1. Schematic experimental apparatus.

3. Results

Fig. 2 depicts a sequence of photographs showing the oblique collision of a water drop with a smooth solid surface when the preimpact diameter of drops,  $D_p$ , is 2.55 mm, and the impact velocity,  $v_0$ , is 1.31 m/s. The upper side of each photograph is the higher side of inclined impact surface, and vice versa. Also, the moment of impact is set to the time  $t = 0$  ms. The measurement accuracy of the time is within plus or minus 0.1 ms for each figure. The horizontal dotted lines indicate the estimated vertical location of the impact point of droplets onto the solid. Although the images are actually taken from the reverse side of the impact surface, they look like bird’s-eye-view photographs due to the reflection of light at the liquid/air interface, as previously explained. Some parts in the liquid/solid contact area (wet area) are very bright. As expected, the liquid/solid contact area increases with time. Since the drop collides with an inclined solid surface, the wet area mainly spreads toward the lower direction. It is well known for the case of normal impact of drops onto a solid surface (for example, Chandra and Avedisian [1]) that a ring structure is formed in the periphery of the drop due to surface tension. The formation of the similar ring structure is clearly seen in the present case ( $t \geq 1.5$  ms).

Under certain conditions, when a drop vertically collides with a horizontal smooth solid surface, some air between the drop and the solid surface is entrapped and then a small bubble is formed at the impact point [3,4].

Similar phenomena are observed in the present results of  $45^\circ$  oblique collision. It should be noted that white points indicated by arrows at  $t = 0.5$  ms and 1.0 ms are bubbles, although the bubble is very small and unclear in the photographs with low magnifications. After the close investigation of many photographs, it was found that the bubble stays at or very close to the impact point, at least until  $t = 5.0$  ms.

The detailed formation process of the bubble is investigated by carefully observing the liquid/solid contact area with higher magnifications just after impact. Fig. 3 displays a sequence of photographs showing the liquid/solid contact area just after the collision. The impact conditions are the same as Fig. 3. Note that the time in every photograph cannot be accurately determined because these events occur in a time scale much shorter than the measurement accuracy of time. These photographs are arranged in chronological order using the fact that the wet area increases with time.

Fig. 3(a) shows that when a drop first contacts the solid surface, it is ring-shaped. Both internal and external boundaries of the ring-shaped wet area are the contact lines, which are defined by the boundary between the air and the liquid at the solid surface. Some air is trapped inside the inner circular contact line. Also, the

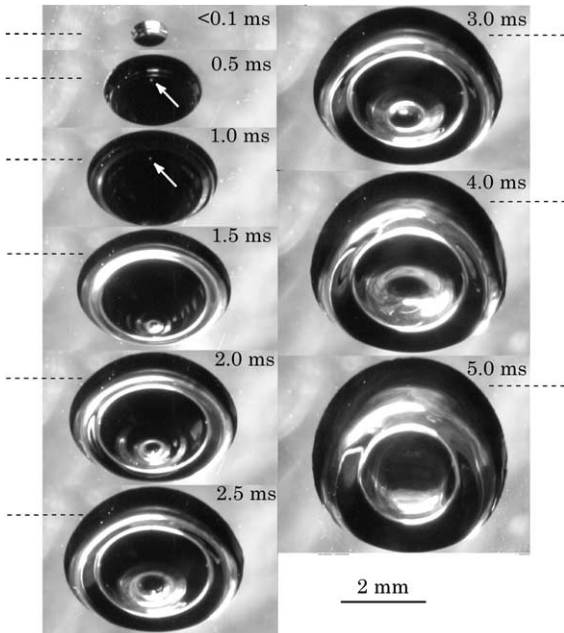


Fig. 2. Time evolution of liquid/solid contact area on the surface just after the collision for impact velocity at 1.31 m/s.

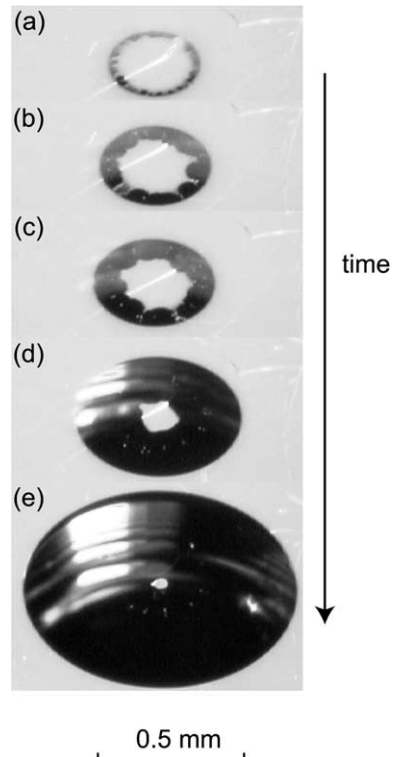


Fig. 3. Entrapment of air at  $45^\circ$  collision for impact velocity at 1.31 m/s.

inner contact line is inequable in azimuthal direction. In (b) and (c), the fingering pattern of the wet area is developed radially inward. As the fingering pattern progresses inward, the liquid/air area (dry area) is reduced. In (d), a non-circular dry area is seen inside the circular wet area. When two front edges of the wet area merge, some air is isolated between these front edges. Coalescence of the front edges often occurs in this time stage. Consequently, several small bubbles appear around the dry area at the impact point. For convenience, such small bubbles are called satellite bubbles. In (e), the fingering pattern no longer exists because every front edge has been merged. The dry area becomes circular, and finally a single bubble is formed at the impact point. The present authors took more than 100 photographs under the same experimental conditions. Such satellite bubbles were always observed, although the number of satellite bubbles was different in each photograph. This is because the fingering pattern of the ring-shaped wet area is not the same at each impact test.

Chandra and Avedisian [1] investigated the deformation process of *n*-heptane droplets vertically impacting onto a horizontal smooth stainless surface. They reported that similar satellite bubbles in a ring surrounding the center bubble appear at relatively high surface temperatures ( $\geq 80$  °C), but the bubble ring was not observed at a low surface temperature ( $= 24$  °C). They concluded that the formation of the bubble ring is not due to the entrapment of air, but due to the cavitation, because the entrap mechanism should not be strongly influenced by the surface temperature. In the present case, the formation of the bubble ring is obviously caused by the entrapment of air. The formation mechanism of satellite bubbles is different from Chandra's results.

Fig. 4 represents the evolution of liquid/solid contact area for the impact velocity at 2.11 m/s. The preimpact diameter of drops is 2.55 mm. The results differ from those of the previous case. Few fingering patterns can be seen within the ring-shaped wet area. Accordingly, no satellite bubbles are formed. A circular dry area decreases when increasing the external diameter of the ring-shaped wet area.

In the present experiments, the drops are formed by a drip method. They are teardrop-shaped at the needle. The falling drops oscillate slightly due to the effect of surface tension. The liquid viscosity reduces oscillation by departing from the needle tip. Therefore, the shape of drops is not a perfect sphere at the moment of oblique impact onto the solid, particularly, in the case of a lower impact velocity. In addition, small disturbances (ripples) might arise at the liquid/air interface due to shear stress when the drops fall in a quiescent air. Asymmetric shape of drops might lead to the formation of the fingering pattern. Incidentally, the pressure of the entrapped air at the impact point just after the collision is higher at a

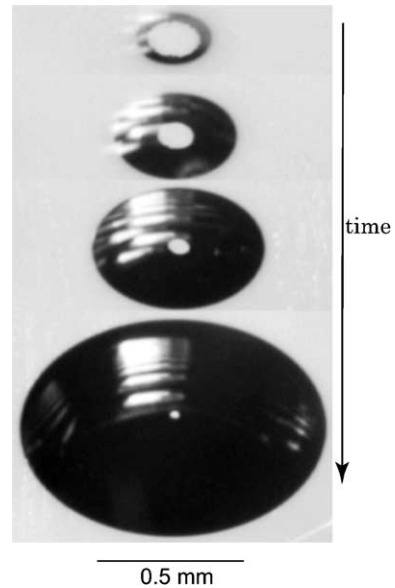


Fig. 4. Entrapment of air at 45° collision for impact velocity at 2.11 m/s.

larger impact velocity. High pressure of the entrapped air is expected to suppress the progress of the fingering pattern. For these reasons, the satellite bubbles are formed for the lower impact velocity, but not formed for the higher velocity.

In order to enrich this discussion, an additional experiment is carried out. Fig. 5 shows the results for the impact velocity at 0.80 m/s. A ring-shaped wet area is observed in (a). Then, some much darker areas appear in the ring-shaped area, as shown in (b). Namely, two types of dark areas exist; relatively dark areas compared to dry areas, and much darker areas. For convenience, the relatively dark areas are called intermediate areas. The latter areas (much darker areas) mean that the liquid is in directly contact with the solid. In later time stages (c) and (d), the intermediate areas cannot be seen. They appear only just after the impact.

Incidentally, the refractive index of air is dependent on the pressure, the vapor pressure and the temperature. However, these effects are negligibly small in the present case. Therefore, the intermediate areas indicate that the water contacts the surface, but the contact feature in molecular scale might be different from that in the much darker area (wet area).

The wet areas in the ring-shaped intermediate area arise asymmetrically and randomly. In (c), the shape of the dry area is very distorted and several satellite bubbles are seen. Subsequently, the dry area at the impact point is reduced and becomes circular as shown in (d). Some satellite bubbles exist near the center bubble, but they are never formed in a ring. The position and the number of satellite bubbles are random.

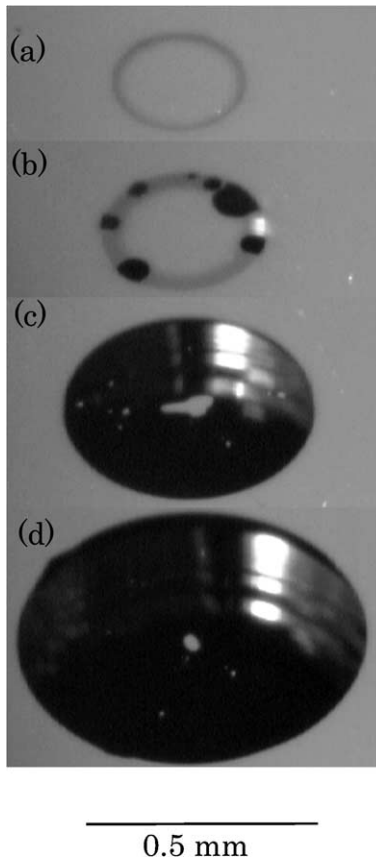


Fig. 5. Entrainment of air at  $45^\circ$  collision for impact velocity at 0.80 m/s.

The experiment of drops impacting normally onto the solid surface is also carried out in the case where preimpact diameter of drops is 2.55 mm, and the impact velocity is 1.31 m/s, to examine the effect of impact angle. The observed entrainment process of air for the normal collision shows similar trends not to the case of Fig. 3, but to the case of Fig. 4. Namely, few fingering pattern is observed inside the ring-shaped wet area and no satellite bubbles are formed. This is due to the dif-

ference of velocity components normal to the solid surface. At  $45^\circ$  oblique collision, the velocity component normal to the solid is 0.92 m/s in case of Fig. 3 and 1.49 m/s in case of Fig. 4.

#### 4. Conclusions

The oblique collision of the water drops with the glass surface was investigated by means of photographic observation. The focus of the study was on the physics of phenomena occurring on the solid surface just after collision. It was found that the drop directly contacts the solid surface in a ring shape, and the entrainment of air between the drop and the solid surface occurs for all cases. When the impact velocity of drops is relatively small, a fingering pattern of wet area is developed radially inward from the internal contact line, resulting in the formation of satellite bubbles. This is probably due to the asymmetric shape of drops. For a relatively high velocity, no satellite bubbles are formed.

#### Acknowledgements

The present authors would like to thank Mr. Satoshi Ito, who was a graduate student at Kyoto University, for his assistance in the experiments.

#### References

- [1] S. Chandra, C.T. Avedisian, On the collision of a droplet with a solid surface, *Proc. R. Soc. London, Ser. A* 432 (1991) 13–41.
- [2] M. Pasandideh-Fard, Y.M. Qiao, S. Chandra, J. Mostaghimi, Capillary effects during droplet impact on a solid surface, *Phys. Fluids* 8 (1996) 650–659.
- [3] S.T. Thoroddsen, J. Sakakibara, Evolution of the fingering pattern of an impacting drop, *Phys. Fluids* 10 (1998) 1359–1374.
- [4] H. Fujimoto, H. Shiraisi, N. Hatta, Evolution of liquid/solid contact area of a drop impinging on a solid surface, *Int. J. Heat Mass Transfer* 43–49 (2000) 1673–1677.